Interfacial and Intrafacial Linkage Isomerizations of Rhenium Complexes with Aromatic Molecules

Benjamin C. Brooks, Scott H. Meiere, Lee A. Friedman, Emily H. Carrig, T. Brent Gunnoe, and W. Dean Harman*

Contribution from the Department of Chemistry, University of Virginia, Charlottesville, Virginia 22901

Received August 28, 2000

Abstract: The mechanisms for the interconversion of facial diastereomers of a variety of TpRe(CO)(L)(η^2-L_{Ar}) complexes {L = ^{t}BuNC, pyridine (py), PMe_3, or 1-methylimidazole (MeIm); L_{Ar} = benzene, anisole, naphthalene, 1-methylpyrrole, furan, or thiophene; Tp = hydridotris(pyrazolyl)borate} have been investigated by ^{1}H NMR spin saturation experiments. In addition, the rates and free energies of activation for these processes were calculated from spin saturation experiments and T_1 measurements. The operative mechanisms for interconversion of the π diastereomers were found to be nondissociative, undergoing either an interfacial or intrafacial linkage isomerization. A comparison of the kinetic parameters for isomerization of related η^2-olefin complexes of the {TpRe(CO)(PMe_3)} and {CpRe(NO)(PPh_3)}$^+$ fragments is also presented.

Introduction

The pentaammineosmium(II) system has proven to be a versatile dearomatization agent for arenes and aromatic heterocycles.[1] This methodology has been applied to benzenes,[2−5] naphthalenes,[6] pyrroles,[7] furans,[8] and thiophenes,[9] resulting in a diverse range of novel organic transformations. A long-standing goal of our research program has been to extend this methodology to chiral transition metal complexes. Our recent discovery of the asymmetric π-base {TpRe(CO)(PMe_3)}[10,11] was the first step toward achieving this goal. Unlike the synthetic procedures established for the pentaammineosmium(II) system,[12] rational design of TpRe systems allows for considerable variation in the ligand set, providing for a variety of novel TpRe(CO)(L)(η^2-L_{Ar}) complexes to be isolated {L = ^{t}BuNC, pyridine (py), PMe_3, and 1-methylimidazole (MeIm); L_{Ar} = benzene, anisole, naphthalene, 1-methylpyrrole, furan, and thiophene}.[13,14]

The η^2 coordination of a prochiral aromatic ligand by a chiral metal can result in both constitutional and stereolinkage isomers, differing in either position or enantioface of binding:

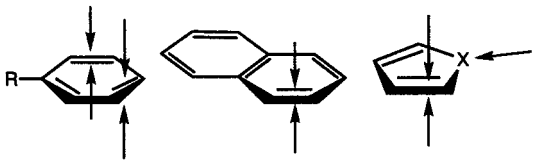

Gladysz and co-workers have extensively investigated the ability of the chiral rhenium Lewis acid {Cp^{x}Re(NO)(PPh_3)}$^+$ (Cp^x = cyclopentadienyl or pentamethylcyclopentadienyl) to bind olefins, aldehydes, and other unsaturated ligands.[15] Particularly relevant to the current study, complexes of the form [CpRe(NO)(PPh_3)(η^2-CH_2=CHR)]$^+$ have been shown to undergo nondissociative interfacial isomerization, a process in which the metal moves from one face of the olefin to the other without decomplexation.[16] Thus, it stands to reason that aromatic ligands bound η^2 to a transition metal might also undergo interfacial isomerizations. Depending on the rate of this process, the stereochemistry of η^2-arene complexation may be governed by thermodynamic rather than kinetic factors. To better understand the chiral recognition of {TpRe(CO)(L)} fragments for aromatic ligands, we set out to characterize those mechanisms responsible for the interconversion of the corresponding linkage isomers and determine the relative rates for these pathways using NMR spectroscopy.

Results

A general method for the preparation of {TpRe(CO)(L)(η^2-L_{Ar})} systems allows for the regulation of both electronic and steric characteristics of the dearomatization agent. By modifying the donor ligand (L), both binding affinity and diastereoselectivity of the metal can be altered. Thus, while the more electron-rich systems (e.g., L = MeIm) bind a full array of aromatic

(1) Harman, W. D. *Chem. Rev.* **1997**, *97*, 1953.
(2) Winemiller, W. D.; Kopach, M. E.; Harman, W. D. *J. Am. Chem. Soc.* **1997**, *119*, 2096.
(3) Chordia, M. D.; Harman, W. D. *J. Am. Chem. Soc.* **1998**, *120*, 5637.
(4) Kolis, S. P.; Gonzalez, J.; Bright, L. M.; Harman, W. D. *Organometallics* **1996**, *15*, 245.
(5) Kopach, M. E.; Harman, W. D. *J. Am. Chem. Soc.* **1994**, *116*, 6581.
(6) Winemiller, M. D.; Harman, W. D. *J. Am. Chem. Soc.* **1998**, *120*, 7835.
(7) Hodges, L. M.; Spera, M. L.; Moody, M.; Harman, W. D. *J. Am. Chem. Soc.* **1996**, *118*, 7117.
(8) Chen, H.; Hodges, L. M.; Liu, R.; Stevens, W. C.; Sabat, M.; Harman, W. D. *J. Am. Chem. Soc.* **1994**, *116*, 5499.
(9) Spera, M. L.; Harman, W. D. *J. Am. Chem. Soc.* **1997**, *119*, 8843.
(10) Gunnoe, T. B.; Sabat, M.; Harman, W. D. *J. Am. Chem. Soc.* **1999**, *121*, 6499.
(11) Gunnoe, T. B.; Sabat, M.; Harman, W. D. *Organometallics* **2000**, *19*, 728.
(12) Lay, P. A.; Magnuson, R. H.; Taube, H. *Inorg. Synth.* **1986**, *24*, 269.
(13) Meiere, S. H.; Brooks, B. C.; Carrig, E. H.; Gunnoe, T. B.; Sabat, M.; Harman, W. D., manuscript in preparation.
(14) Meiere, S. H.; Brooks, B. C.; Gunnoe, T. B.; Sabat, M.; Harman, W. D. *Organometallics*, in press.
(15) Gladysz, J. A.; Boone, B. J. *Angew. Chem., Int. Ed. Engl.* **1997**, *36*, 550.
(16) Peng, T.-S.; Gladysz, J. A. *J. Am. Chem. Soc.* **1992**, *114*, 4174.

10.1021/ja003195j CCC: $20.00
Published on Web 03/21/2001

Table 1. Equilibrium Constants and Diastereoselectivities of TpRe(CO)(L)(η^2-L_{Ar}) Systems

$$\text{minor diastereomer} \underset{k_{-1}}{\overset{k_1}{\rightleftharpoons}} \text{major diastereomer}$$
$$K_{eq}=k_1/k_{-1}$$

compound	K_{eq}	T (K)	quadrant in which R or X of major isomer is found[a]
TpRe(CO)(^{t}BuNC)(η^2-furan) (**1**)	2.2	273	A
TpRe(CO)(^{t}BuNC)(η^2-2-methylfuran) (**2**)	4.9	298	A
TpRe(CO)(^{t}BuNC)(η^2-thiophene) (**3**)	4.3[b]	273	A
TpRe(CO)(^{t}BuNC)(η^2-naphthalene) (**4**)	1.2	273	D
TpRe(CO)(^{t}BuNC)(η^2-2-methoxy-naphthalene) (**5**)	1.0	308	A
TpRe(CO)(^{t}BuNC)(η^2-1,8-dimethyl-naphthalene) (**6**)	1.2	293	D
TpRe(CO)(PMe_3)(η^2-furan) (**7**)	2.1	323	A
TpRe(CO)(PMe_3)(η^2-thiophene) (**8**)	1.6[c]	323	A
TpRe(CO)(PMe_3)(η^2-naphthalene) (**9**)	>19	323	A
TpRe(CO)(py)(η^2-furan) (**10**)	1.6	323	A
TpRe(CO)(py)(η^2-thiophene) (**11**)	1.2	323	D
TpRe(CO)(py)(η^2-naphthalene) (**12**)	3.0	323	D
TpRe(CO)(MeIm)(η^2-furan) (**13**)	1.4	343	D
TpRe(CO)(MeIm)(η^2-thiophene) (**14**)	1.0	343	D
TpRe(CO)(MeIm)(η^2-naphthalene) (**15**)	4.5	343	D
	>20	253	D
TpRe(CO)(MeIm)(η^2-benzene) (**16**)	na[d]	na	na
TpRe(CO)(MeIm)(η^2-anisole) (**17**)	3.0	293	D
TpRe(CO)(MeIm)(η^2-1-methyl-pyrrole) (**18**)	6.0	178	D

[a] See Scheme 1. [b] K_{eq} refers to η^2:η^2 diastereomers (S-bound isomer also observed with η^2-bound to S-bound ratio = 1.2:1). [c] K_{eq} refers to η^2:η^2 diastereomers (S-bound isomer also observed with η^2-bound to S-bound ratio = 5.2:1). [d] na, not applicable.

ligands (e.g., benzenes, pyrroles, furans, thiophenes, and naphthalenes), the less electron-rich systems (e.g., L = ^{t}BuNC, PMe_3, and py) form stable complexes only with furans, naphthalenes, and thiophenes. The regiochemistry of aromatic coordination is governed largely by electronic factors and is entirely consistent with that observed for pentaammineosmium-(II).[1] Thus, the heterocycles furan, pyrrole, and thiophene are coordinated across C2 and C3, naphthalene is bound across C1 and C2, and anisole is bound across C2 and C3.

In Table 1, the major stereoisomer for each of a variety of TpRe(CO)(L)(η^2-L_{Ar}) complexes is categorized according to which quadrant the heteroatom or substituent (R) is located (Scheme 1). The equilibrium constants listed in Table 1 correspond to the ratio of major to minor diastereomers, and by this definition they are always greater than or equal to unity. Electronic constraints dictate that the coordinated double bond of the aromatic ligand be orthogonal to the carbonyl ligand.[11] For the {TpRe(CO)(MeIm)} system, quadrant C has been found to be the most sterically congested quadrant, followed by (in order) quadrants B, A, and D (Scheme 1).[17] In all cases observed, the coordinated ring is oriented toward the CO ligand and extends into quadrants A and D. Steric interactions with the pyrazole ring trans to the CO destabilize the conformers (i.e., rotamers) in which the aromatic ring extends into quadrant B or C. However, these BC rotamers are likely to be kinetically accessible on the basis of recent studies of related olefin complexes of these TpRe systems. Specifically, activation energies for rotation in the corresponding TpRe(CO)(L)(η^2-ethylene) complexes have been determined to range from 7 to 13 kcal/mol.[18] Moreover, spectroscopic evidence for BC rotamers has been obtained for some dihydrofuran systems of the {TpRe(CO)(L)} fragments.[19] Some of the isomers reported in this study show broadened resonances in the proton NMR spectrum at ambient temperature that are likely due to a hindered rotation about the aromatic−metal bond. However, in no case has lowering the temperature revealed detectable amounts of any BC rotamer.[10,11]

Scheme 1. General Schematic Description of Selectivity Issues for TpRe(CO)(L)(η^2-L_{Ar}) Systems

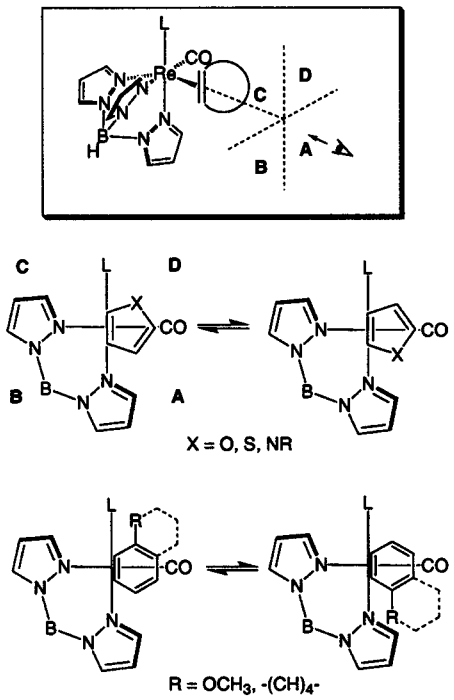

For the most part, diastereoselectivity for complexes of aromatic ligands is poor, owing to the lack of significant steric differentiation (Table 1). Nevertheless, several {TpRe(CO)(L)} fragments do exhibit moderate diastereoselectivity for certain aromatic ligands. For example, the imidazole system {TpRe-(CO)(MeIm)} binds naphthalene (dr > 20:1 at −20 °C), 1-methylpyrrole (dr = 6:1 at −95 °C), and 2,6-lutidine (dr > 7:1 at −20 °C) with moderate stereocontrol.[14] Additionally, the {TpRe(CO)(PMe_3)} system has been shown to coordinate naphthalene as a single diastereomer.[10] Given that the coordinated double bond of the aromatic ligand is orthogonal to the carbonyl ligand,[11] stereoselectivity is determined by the relative steric interactions of L and the pyrazole ring trans to this ligand with a ring substituent (R) or uncoordinated ring (e.g., naphthalene) of the aromatic system.

Resonances in the ^{1}H NMR spectrum for each diastereomer of a particular compound were assigned utilizing the anisotropic shifts caused by the pyrazolyl moiety of the Tp ligand, as well as ^{1}H−^{1}H COSY data. As previously reported,[11] these assignments have been rigorously defined for the TpRe(CO)(PMe_3)-(η^2-L_{Ar}) systems according to NOE data as well as phosphorus−hydrogen coupling information. Extrapolation of the upfield shifts caused by the Tp ligand for protons in quadrant B (see

(17) Meiere, S. H.; Harman, W. D. Manuscript in preparation.

(18) Friedman, L. A.; Brooks, B. C.; Meiere, S. M.; Harman, W. D. *Organometallics* **2001**. In press.

(19) Friedman, L. A.; Harman, W. D. Submitted for publication.

Scheme 2. Expected Spin Saturation Exchanges for Dihapto-Coordinated Arene Ligands of {TpRe(CO)(L)} Systems

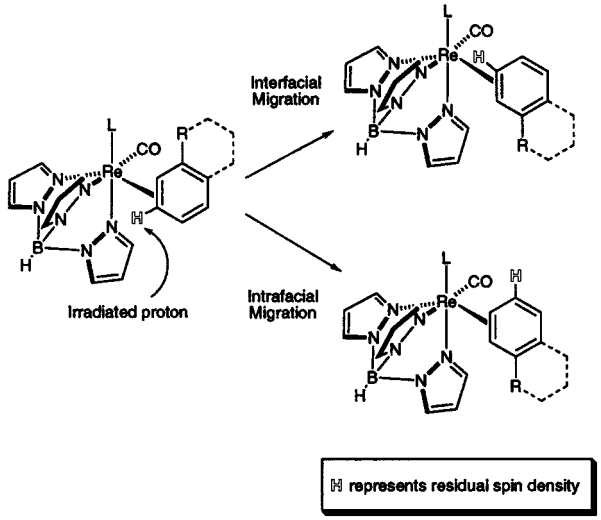

Scheme 1) coupled with NOE and 2D NMR techniques has allowed for general assignments of all {TpRe(CO)(L)} systems.

Rate Measurements. Spin saturation experiments have provided a useful method for analyzing which mechanisms are operative for the interconversion of facial diastereomers. Similar EXSY experiments[20] would have afforded the same information; however, the wide spectral windows, large T_1 values (3−15 s), and various temperatures required for many of the {TpRe(CO)(L)} systems rendered the one-dimensional technique more convenient.

Two nondissociative processes can be envisioned for the interconversion of diastereomers of coordinated arenes shown in Scheme 1. Isomerization may occur through either an interfacial isomerization (i.e., a face-flip) or an intrafacial isomerization (i.e., a ring-walk). Thus, an interfacial migration involves the isomerization of the metal to the opposite enantioface of the originally coordinated double bond. In contrast, an intrafacial migration requires movement of the metal to an originally uncoordinated double bond on the same face of the arene. Significantly, although the product is identical for all of the complexes examined, these pathways result in the interconversion of different protons, as shown in Schemes 2 and 3. Thus, the existence of either mechanism for isomerization can be elucidated by identification of the protons involved in spin saturation exchange. For aromatic heterocycles, the randomization of intrafacial and interfacial migrations becomes possible through the metal binding the heteroatom. Such an action would scramble the spin density of an irradiated proton equally to both sides of the ring, provided that there is rapid bond rotation of the metal−heteroatom bond for the η^1-intermediate and either a planar geometry or rapid inversion at the heteroatom.

Spin saturation experiments also provided a convenient method to obtain rate data for the interconversion of diastereomers of each TpRe(CO)(L)(η^2-L_{Ar}) system. Thus, the rate of exchange for each mechanism was determined by measuring the decrease in signal intensity for the peak in question after irradiation of its exchange partner and comparing that to the intensity of the same peak without irradiation. In addition, the observed spin−lattice relaxation times (T_1) for the various peaks observed in the spin saturation experiment were obtained. From

(20) Perrin, C. L.; Dwyer, T. L. *Chem. Rev.* **1990**, *90*, 935.

Scheme 3. Expected Spin Saturation Exchanges for Dihapto-Coordinated Aromatic Heterocycle Ligands of {TpRe(CO)(L)} Systems

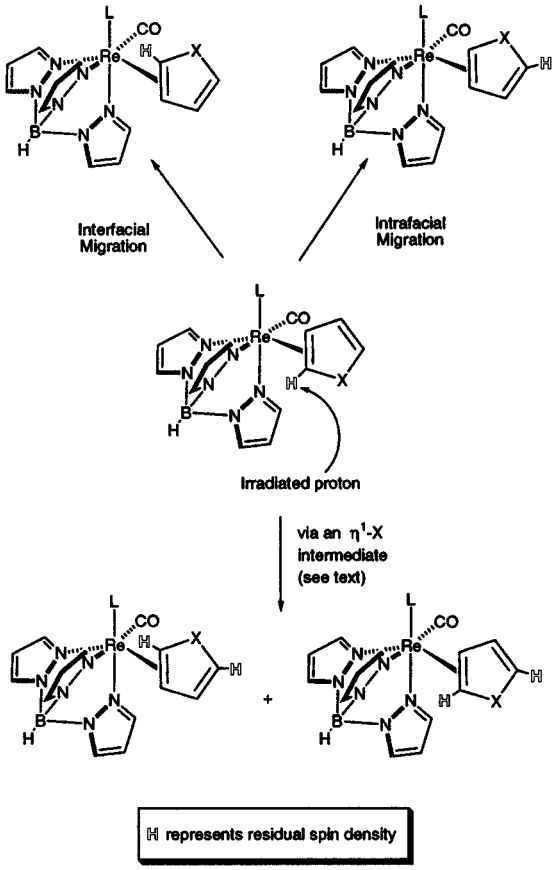

these data, the rate was calculated utilizing the Forsén−Hoffman relation (eq 1):[21−24]

$$k = \frac{1}{T_1}\left(\frac{M(0)}{M(\infty)} - 1\right) \qquad (1)$$

where $M(0)$ is the observed peak intensity before saturation, $M(\infty)$ is the intensity of the same peak after saturation, and T_1 is the apparent spin−lattice relaxation time of the peak in which saturation is observed.[25] In each case, the rate that was measured corresponds to the migration of the minor diastereomer to the major diastereomer (k_1 as defined in Table 1) for a given mechanism (vide infra). The reverse rate may be obtained using the equilibrium constants listed in Table 1 (where the temperature is the same). The activation barriers (in kilocalories per mole) were then calculated utilizing a variation of the Eyring equation (eq 2):

$$\Delta G^{\ddagger} = (4.575 \times 10^{-3})(T)\left[10.319 + \log\left(\frac{T}{k}\right)\right] \qquad (2)$$

where T is the temperature on the Kelvin scale.[26] In certain

(21) Forsén, S.; Hoffman, R. A. *J. Chem. Phys.* **1963**, *19*, 2892.
(22) Forsén, S.; Hoffman, R. A. *J. Chem. Phys.* **1964**, *40*, 1189.
(23) Hoffman, R. A.; Forsén, S. *Progress in NMR Spectroscopy*; Pergamon Press: Oxford, England, 1966; Vol. 1, p 15.
(24) Faller, J. W. In *Determination of Organic Structure by Physical Methods*; Nachod, F. C., Zuckerman, J. J., Eds.; Academic Press: New York, 1973; Vol. V, p 75.
(25) Mann, B. E. In *Annual Reports on NMR Spectroscopy*; Webb, G. A., Ed.; Academic Press: London, 1982; Vol. 12, p 263.
(26) Sandström, J. *Dynamic NMR Spectroscopy*; Academic Press: New York, 1982.

Table 2. Observed Rates and Activation Barriers for Diastereomeric Interconversion of TpRe(CO)(L)(η^2-L_{Ar}) Systems

	interfacial migration			intrafacial migration		
compound	T_{inter} (K)	$k_{1(inter)}$ $\times 10^{-2}$ (s^{-1})[a]	$\Delta G_{inter}^{\ddagger}$ (kcal/mol)[b]	T_{intra} (K)	$k_{1(intra)}$ $\times 10^{-2}$ (s^{-1})[a]	$\Delta G_{intra}^{\ddagger}$ (kcal/mol)[b]
TpRe(CO)(^{t}BuNC)(η^2-furan) (**1**)	273	56.2	16.2	273	0.212	18.0
TpRe(CO)(^{t}BuNC)(η^2-2-methylfuran) (**2**)	298	107	17.4			
TpRe(CO)(^{t}BuNC)(η^2-thiophene) (**3**)[c]	273	18.3	16.9	273	17.2	16.9
TpRe(CO)(^{t}BuNC)(η^2-naphthalene) (**4**)		<1	>18.4	273	278	15.4
TpRe(CO)(^{t}BuNC)(η^2-2-methoxynaphthalene) (**5**)		<1	>20.8			
TpRe(CO)(^{t}BuNC)(η^2-1,8-dimethylnaphthalene) (**6**)	293	54.6	17.5			
TpRe(CO)(PMe_3)(η^2-furan) (**7**)	323	91.8	19.0	323	1.37	21.7
TpRe(CO)(PMe_3)(η^2-thiophene) (**8**)[d]	323	98.8	19.0	323	19.4	20.0
TpRe(CO)(PMe_3)(η^2-naphthalene) (**9**)	na	na	na	na	na	na
TpRe(CO)(py)(η^2-furan) (**10**)	323	5.01	20.9		<1	>21.9
TpRe(CO)(py)(η^2-thiophene) (**11**)	323	4.44	21.0	323	1.12	21.9
TpRe(CO)(py)(η^2-naphthalene) (**12**)		<1	>21.9	323	12.4	20.3
TpRe(CO)(MeIm)(η^2-furan) (**13**)	343	2.18	22.8		<1	>23.3
TpRe(CO)(MeIm)(η^2-thiophene) (**14**)	343	1.53	23.0		<1	>23.3
TpRe(CO)(MeIm)(η^2-naphthalene) (**15**)		<1	>23.3	343	3.41	22.5
TpRe(CO)(MeIm)(η^2-benzene) (**16**)[e]				233	1.14	14.5
TpRe(CO)(MeIm)(η^2-anisole) (**17**)[f]	293	20.0	18.1	293	84.8	17.2
TpRe(CO)(MeIm)(η^2-1-methylpyrrole) (**18**)[g]				213	65.5	10.6

[a] k_1 is the rate of migration from the minor diastereomer to the major diastereomer as defined in Table 1; errors in rates are estimated to be ±5%. [b] Errors in $\Delta G^{\ddagger}$ are estimated to be ±0.3 kcal/mol. [c] Observed spin saturation exchange with S-bound isomer. [d] Observed no spin saturation exchange with S-bound isomer. [e] Refers to migration from 1,2-η^2 to 2,3-η^2 isomer. [f] Refers to migration from 2,3-η^2 to 5,6-η^2 isomer. [g] Measured using coalescence data of bound protons (see eq 3).

instances where coalescence could be observed, the frequency was also used to obtain the rate according to eq 3:

$$k = \frac{(\Delta\nu)\pi}{\sqrt{2}} \tag{3}$$

where $\Delta\nu$ represents the difference in frequency between the two observed peaks at the slow exchange limit. The activation barrier was then calculated using the coalescence temperature (T_c) and eq 2.

Results of Spin Saturation Measurements. The rates and free energies of activation measured using the spin saturation data are summarized in Table 2. These rates correspond to the migration from the minor to the major diastereomer (k_1) and are listed according to mechanism and {TpRe(CO)(L)} system. In the case of TpRe(CO)(MeIm)(η^2-benzene) (**16**), the rate listed refers to intrafacial migration of the metal to the bond adjacent to the originally coordinated double bond. In contrast, the rate measured for intrafacial migration of the anisole complex **17** refers to an isomerization between the 2,3-η^2 to 5,6-η^2 forms.

A range of temperatures was required to obtain these data due to the differing electronic characteristics of the {TpRe(CO)(L)} fragments and the nature of the aromatic ligands (L_{Ar}). Investigation of aromatic complexes of the less electron-rich systems (e.g., the {TpRe(CO)(^{t}BuNC)} fragment) was limited by the thermal instability of these compounds at higher temperatures. The parent furan, thiophene, and naphthalene complexes of the isonitrile system (**1**, **3**, and **4**) exhibit fluxional ^{1}H NMR spectra at 20 °C. Accordingly, these complexes were analyzed at lower temperatures (between −20 and 10 °C). By utilizing substituted furan (**2**) and naphthalene systems (**5** and **6**), this fluxionality was inhibited. This observation indicates that the rapid interconversion of the parent systems is due to intrafacial migrations at room temperature. By inhibiting this process using the methylated analogues **2** and **6**, the slower interfacial isomerizations were qualitatively identified for the parent complexes. In contrast to the furan complexes of the isonitrile system, the presence of the methyl group in the complex TpRe(CO)(^{t}BuNC)(4,5-η^2-2-methylthiophene) does not deter fluxional behavior at 20 °C.

Whereas the major isomers for the furan, thiophene, and naphthalene complexes of the {TpRe(CO)(MeIm)} system appear static in the proton NMR spectrum, the spectra of the benzene and 1-methylpyrrole complexes of the {TpRe(CO)(MeIm)} fragment (**16** and **18**) are severely broadened at 20 °C. The ^{1}H NMR spectrum of complex **18** is fluxional at temperatures as low as −90 °C. Accordingly, coalescence of the bound proton signals was utilized in order to obtain rate information for this system (see eq 3).

The activation barriers for the interfacial migration of two olefinic complexes TpRe(CO)(PMe_3)(η^2-2,3-dihydrofuran) (**19**) and TpRe(CO)(PMe_3)(η^2-2β,5β-dideuterio-2,5-dihydrofuran) (**20**) have been measured.[19] The facial diastereomers of **19** were separated using chromatographic methods. Monitoring the equilibration of the diastereomers by ^{1}H NMR (at elevated temperatures for complex **20**) allowed for measurement of the specific rate for the interconversion of the facial diastereomers. The free energies of activation were found to be 25.6 (25 °C) and 30.3 kcal/mol (75 °C) for **19** and **20**, respectively.

Discussion

A variety of intermediates can be invoked to explain the interfacial isomerizations for aromatic heterocycles (Scheme 4) and for arenes (Scheme 5). First, the metal can dissociate from the aromatic ligand and then recoordinate in order to form a coordination diastereomer (pathway I). However, a dissociative isomerization pathway may be ruled out for these systems since proton NMR experiments were performed in a solvent (acetone-d_6) which binds faster and forms more thermodynamically stable complexes than the aromatic ligand of interest (unpublished substitution data). Furthermore, if the interconversion of facial diastereomers were dissociative, one would observe scrambling of all irradiated protons in both diastereomers, which does not occur. Finally, independent experiments verify that the benzene ligand in the complex TpRe(CO)(MeIm)(benzene)[14] does not undergo rapid exchange with the solvent benzene-d_6 on the time scale of its linkage isomerizations.

Alternatively, the complex can isomerize through nondissociative pathways. For instance, the metal can shift to a

Scheme 4. Possible Pathways and Intermediates for Interfacial Migration of Aromatic Heterocycles[a]

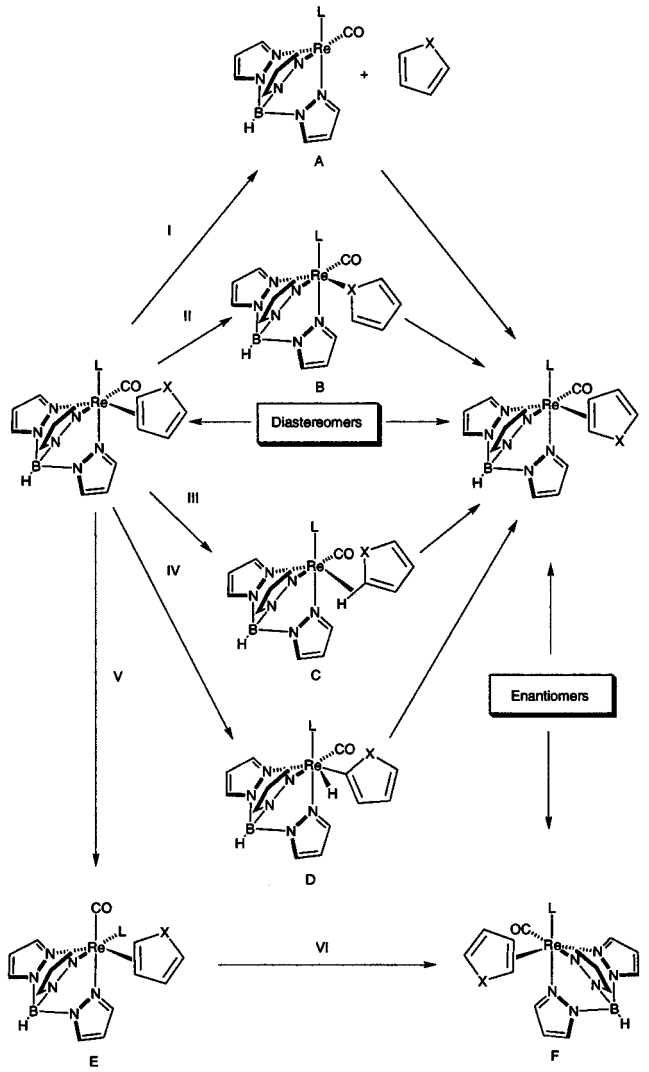

[a] Species A, dissociated intermediate; species B, heteroatom-bound intermediate; species C, C−H σ-bound intermediate; species D, arylhydrido intermediate; species E, rhenium inversion intermediate; species F, enantiomer of the product diastereomer.

heteroatom (i.e., a "conducted tour" mechanism, pathway II),[27,28] swing through the π-nodal plane of the aromatic ligand by turning on a C−H σ bond (pathway III; agostic interaction), or form an aryl hydride intermediate (pathway IV; oxidative addition). We note that pathways III and IV are actually two limiting cases describing the three-center interaction between the rhenium, carbon, and hydrogen. Finally, the interfacial migration can occur through an inversion of metal configuration (e.g., CO and L switch places; pathway V) followed by metal−aromatic bond rotation (pathway VI) to give an enantiomer (F) of the other diastereomer. Inversion of the rhenium center seems unlikely since Gladysz did not observe such an interconversion for the similar $[CpRe(NO)(PPh_3)(\eta^2\text{-}CH_2{=}CHR)]^+$ systems.[16] Furthermore, preliminary results from our laboratory indicate that α-pinene can be used to resolve enantiomers of the {TpRe(CO)(MeIm)} system and that the rhenium configuration remains intact even at elevated temperatures.[17]

For an intrafacial process, the metal moves from the originally coordinated double bond to another double bond while maintaining the same binding face. In the case of benzene, adjacent dihapto coordination sites are isoergic (e.g., 1,2-η^2 to 2,3-η^2). Like the interfacial migration, the metal can move via a C−H bond (Scheme 5, pathway VIII) or an aryl hydride (vide supra) (pathway IX), but without the bond rotation. Several unique intermediates also exist for the intrafacial migration (Scheme 6). The metal can ring-walk via either an η^1-arene intermediate (pathway XII) or an η^3-allyl species (pathway XIII). Graham et al. have postulated an arenium intermediate for the migration of the benzene ligand in $[CpRe(CO)(NO)(\eta^2\text{-benzene})]^+$.[29,30] In other aromatic systems (e.g., aromatic heterocycles, naphthalenes, and substituted benzenes) the situation becomes even more complex in that adjacent dihapto coordination sites differ in energy yet are likely to be on the reaction pathway. Three relevant examples of this are shown in Scheme 7. In order for the metal to arrive at a chemically equivalent position, it must pass through two or more higher energy intermediates (i.e., those listed above) and at least one lower energy dihapto-coordinated intermediate.

Interfacial Migrations. The free energies of activation for the interfacial migration of olefin complexes $TpRe(CO)(PMe_3)(\eta^2\text{-}2,3\text{-dihydrofuran})$ (**19**) and $TpRe(CO)(PMe_3)(3,4\text{-}\eta^2\text{-}2\beta,5\beta\text{-dideuterio-}2,5\text{-dihydrofuran})$ (**20**) have been determined to be 25.6 (25 °C) and 30.3 kcal/mol (75 °C), respectively. The corresponding values reported by Gladysz et al. for the $[CpRe(NO)(PPh_3)(\eta^2\text{-alkene})]^+$ systems are approximately 30 kcal/mol at 100 °C.[16] Accordingly, these olefinic rhenium systems have free energies of activation for interfacial migration which are 7−15 kcal/mol higher than those observed for complexes of aromatic ligands (see Table 2). For example, complexes **19** and **20** exhibit $\Delta G^{\ddagger}$ values for a face-flip 6−10 kcal/mol greater than the values for the analogous $TpRe(CO)(PMe_3)(\eta^2\text{-furan})$ complex **7**. This large difference in activation free energy for a face-flip between aromatic complexes and olefinic complexes can be attributed to the increase in aromatic character experienced in the heteroatom, C−H σ-bond[31] or aryl hydride intermediates (Scheme 4, pathway II, III, or IV) for the former. Thus, according to the Hammond postulate, the transition state for an intrafacial isomerization is expected to be stabilized relative to the ground state for aromatic complexes more so than for olefinic systems (Scheme 8). From a different perspective, the complex of an aromatic molecule is higher in energy than is that of an olefin (Scheme 8), as a result of the disruption of aromaticity upon binding. This notion is illustrated in Scheme 8 for the case in which furan and dihydrofuran complexes **7**, **19**, and **20** are compared, and a C−H σ-bound complex is arbitrarily chosen as the intermediate. Of note, alkane σ-complexed intermediates have been observed[32,33] and are estimated to be 10−15 kcal/mol more stable than the dissociated hydrocarbons.[34] Again, we note that the C−H-activated intermediates (C and H, Schemes 4 and 5) and aryl hydride intermediates (D and I) proposed represent the extremes of a continuum describing the interaction of a metal and C−H bond.[32,33] The key observation here is that η^2-bound aromatic heterocycle complexes have a lower free energy of activation for interfacial

(27) Ford, W. T.; Cram, D. J. *J. Am. Chem. Soc.* **1968**, *90*, 2606.
(28) Kegley, S. E.; Walter, K. A.; Bergstrom, D. T.; MacFarland, D. K.; Young, B. G.; Rheingold, A. L. *Organometallics* **1993**, *12*, 2339.
(29) Sweet, J. R.; Graham, W. A. G. *J. Am. Chem. Soc.* **1983**, *105*, 305.
(30) Sweet, J. R.; Graham, W. A. G. *Organometallics* **1983**, *2*, 135.
(31) Geftakis, S.; Ball, G. E. *J. Am. Chem. Soc.* **1998**, *120*, 9953.
(32) Bromberg, S. E.; Yang, H.; Asplund, M. C.; Lian, T.; McNamara, B. K.; Kotz, K. T.; Yeston, J. S.; Wilkens, M.; Frei, H.; Bergman, R. G.; Harris, C. B. *Science* **1997**, *278*, 260.
(33) Evans, D. R.; Drovetskaya, T.; Bau, R.; Reed, C. A.; Boyd, P. D. W. *J. Am. Chem. Soc.* **1997**, *119*, 3633.
(34) Hall, C.; Perutz, R. N. *Chem. Rev.* **1996**, *96*, 3125.

Scheme 5. Possible Pathways and Intermediates for Interfacial Migration of Arenes[a]

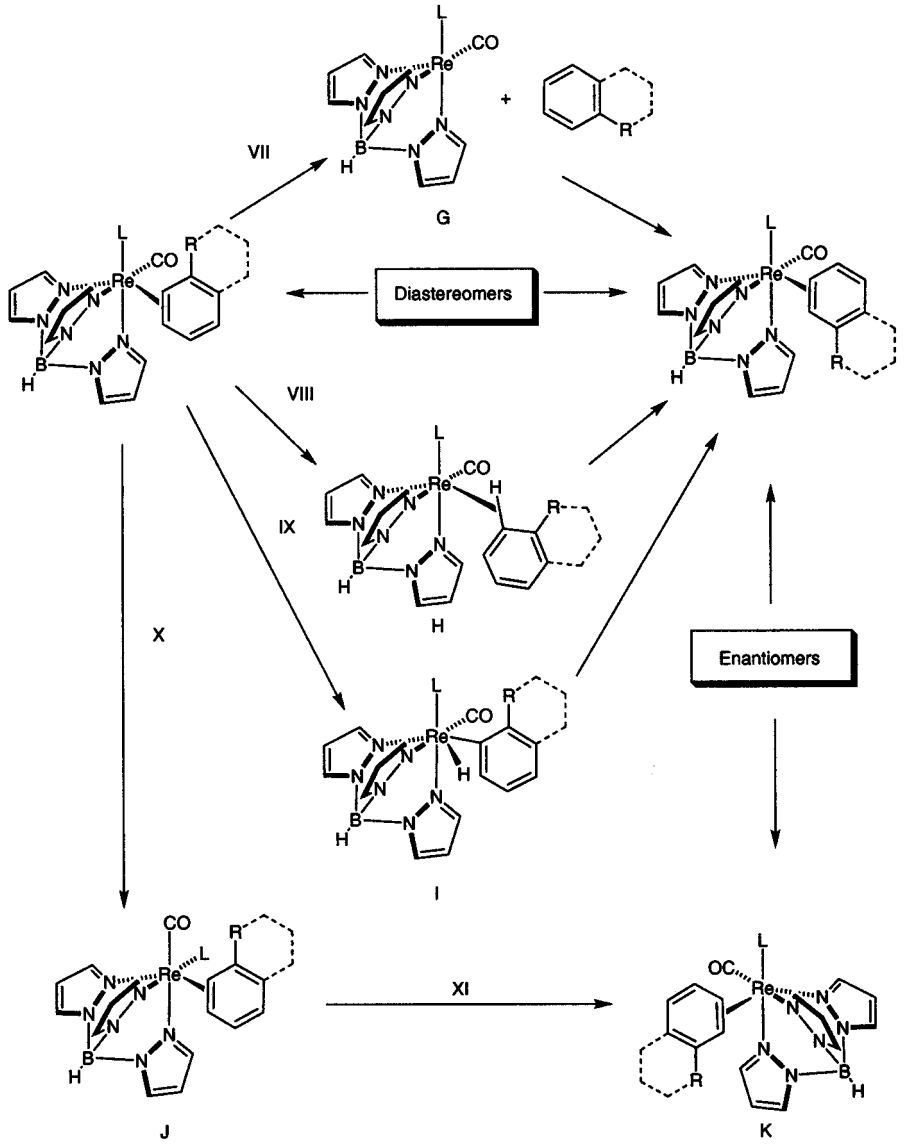

[a] Species G, dissociated intermediate; species H, C−H σ-bound intermediate; species I, arylhydrido intermediate; species J, rhenium inversion intermediate; species K, enantiomer of the product diastereomer.

isomerization than is observed with olefins, and this holds true for η^2-arene complexes as well. A reaction coordinate diagram for arenes could be envisioned to look similar to that shown in Scheme 8 for heterocyclic ligands.

The observed activation energies for each family of {TpRe(CO)(L)} strongly correlate with the electronic nature of each metal center. Thus, for a given aromatic ligand and isomerization, the {TpRe(CO)(^{t}BuNC)} fragment exhibits the smallest values for $\Delta G^{\ddagger}$, followed by {TpRe(CO)(PMe_3)}, {TpRe(CO)(py)}, and {TpRe(CO)(MeIm)}. On the basis of both CO stretching frequencies and electrochemical data, it is concluded that this series moves from the least to the most electron-rich metal center. Plots of the free energy of activation for the interfacial migration for the furan complexes (**1**, **7**, **10**, **13**) versus both the reduction potential (actually $E_{p,a}$ at 100 mV/s) and the carbonyl stretching frequency afford a smooth linear progression (Figure 1). This trend is a direct result of the greater π back-bonding for the more electron-rich systems resulting in a stronger η^2-bond. As L becomes a better donor (or worse π-acceptor), electron density on the metal is increased. Of note, this graph compares free energies of activation at several different temperatures. Presumably, this trend is primarily a reflection of the variation of $\Delta H^{\ddagger}$ as a function of L. Thus, we assume here that $T\Delta S^{\ddagger}$ is only a minor component of $\Delta G^{\ddagger}$ for these processes, or that the entropic contribution to the free energies of activation is roughly the same from system to system. Attempts to determine $\Delta S^{\ddagger}$ and $\Delta H^{\ddagger}$ for any of the TpRe(CO)(L)(η^2-L_{Ar}) systems were frustrated by the narrow range of temperatures at which rates could be determined due to the relative stability of the TpRe aromatic systems; however, similar CpRe olefin systems involved in nondissociative interconversions demonstrated small entropies of activation (2 ± 2 eu for the complex $[CpRe(NO)(PPh_3)(\eta^2\text{-}CH_2{=}CHPh)]^+$).[16]

The TpRe(CO)(^{t}BuNC)(η^2-thiophene) (**3**) and TpRe(CO)(PMe_3)(η^2-thiophene) (**8**) systems show a striking difference in the observed intermediates for both interfacial and intrafacial mechanisms. Both complexes exhibit η^1-S-bound isomers in their ^{1}H NMR spectra at 20 °C. The values of $\Delta G^{\ddagger}$ for both the interfacial and intrafacial migrations for TpRe(CO)(^{t}BuNC)(η^2-thiophene) (**3**) are identical, while the same values for TpRe(CO)(PMe_3)(η^2-thiophene) (**8**) differ by 1 kcal/mol. Complex **3** exhibits spin saturation exchange between the η^2- and η^1-

Scheme 6. Unique Pathways and Intermediates for Intrafacial Migration of TpRe(CO)(L)(η^2-benzene)[a]

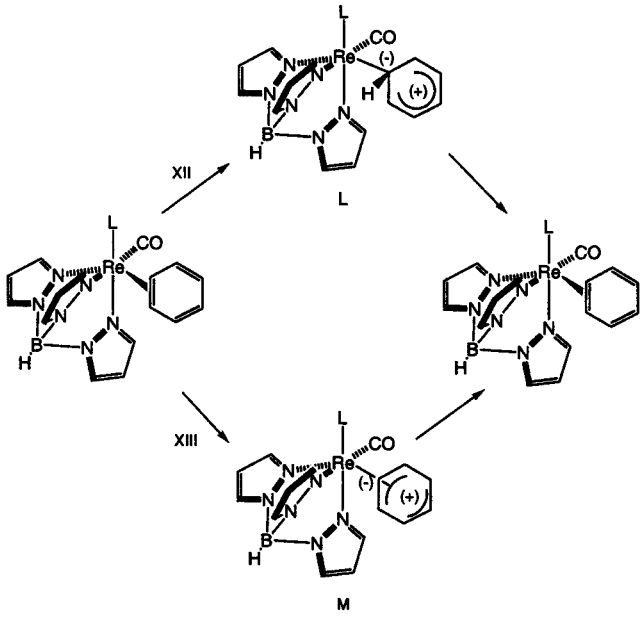

[a] Species L, η^1-intermediate; species M, η^3-allyl intermediate.

bound isomers, whereas complex **8** shows spin saturation exchange only between η^2-bound isomers. In addition, scrambling of all α proton signals was observed for **3** upon irradiation of a single α proton, while this was not seen for **8**. Accordingly, we conclude that whereas it is possible that the S-bound species is an intermediate in the migration of thiophene for many of these systems, in at least one case (**8**) and possibly others, the S-bound isomer *does not lie on the lowest free energy reaction coordinate between interfacial or intrafacial isomers (at least at 50* °C). As one of our reviewers points out, thiophene, when coordinated to a metal in η^1-fashion, is canted due to the partial rehybridization of the sulfur atom from sp^2 to almost sp^3.[35,36] Given this notion, it is conceivable that an η^2-thiophene complex could undergo intrafacial migration through the heteroatom without undergoing an interfacial migration. In the case of **8**, however, *both* inter- and intrafacial processes occur more readily than does the migration of the metal to the heteroatom.

For a given {TpRe(CO)(L)} system, complexes of aromatic molecules show free energies of activation for interfacial isomerization that are very similar, at least where such values were obtained. Given the large difference between the rate of interfacial isomerization for olefins and aromatics, one might expect to see a correlation between the resonance energy for the free arene and the rate of face-flip. Unfortunately, complexes of aromatic molecules with the greatest resonance stabilization energy (i.e., benzene and pyrrole) have fast rates of intrafacial isomerization that pre-empt the facile measurement of the face-flip mechanism. Attempts to block the intrafacial isomerization with methyl substituents (vide supra) render the arene too sterically hindered to form a stable complex. Indeed, the only arene for which the face-flip could be measured was the 1,8-dimethylnaphthalene complex TpRe(CO)(^{t}BuNC)(3,4-η^2-1,8-dimethylnaphthalene) (**6**). Importantly, this system provides an example of an interfacial migration of an arene without the presence of a heteroatom.

(35) Choi, M.-G.; Angelici, R. J. *Organometallics* **1991**, *10*, 2436.
(36) Rincón, L.; Terra, J.; Guenzburger, D.; Sánchez-Delgado, R. A. *Organometallics* **1995**, *14*, 1292.

Scheme 7. Intrafacial Migration of TpRe(CO)(L)(η^2-L_{Ar}) Systems Which Contain Inequivalent Binding Sites Showing Low-Energy Dihapto-Coordinated Intermediates

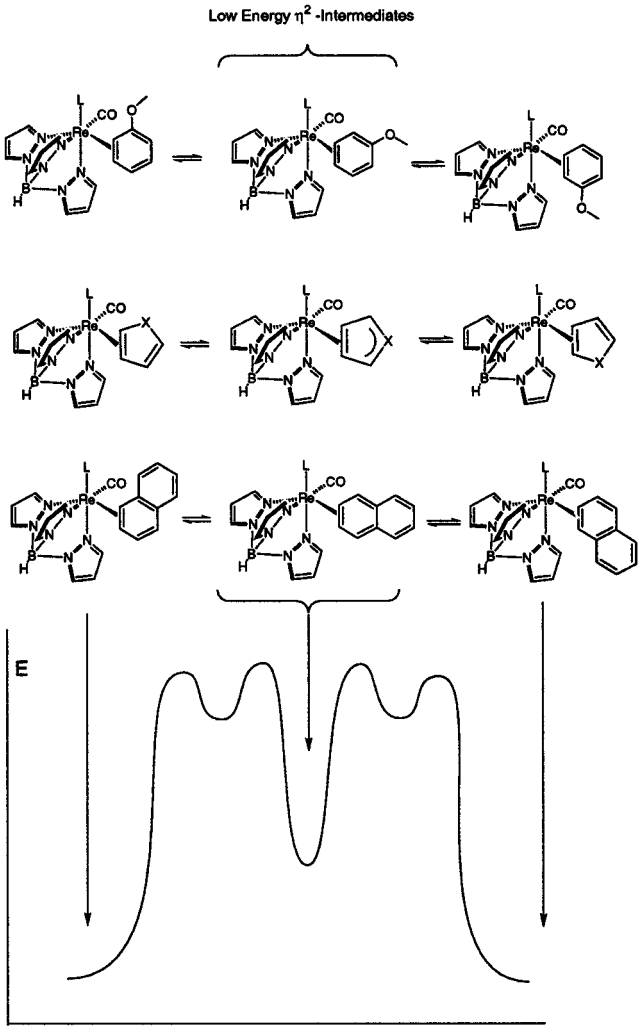

Scheme 8. Comparison of Energetics of Interfacial Migrations for Olefin and Aromatic Heterocycle Complexes of the {TpRe(CO)(PMe_3)} Fragment (M)

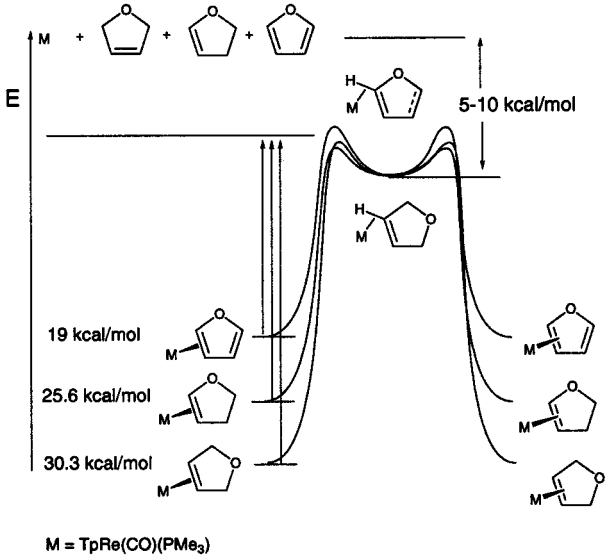

In the case of the TpRe(CO)(^{t}BuNC)(3,4-η^2-2-methoxynaphthalene) complex (**5**), the abnormally high barrier to interfacial

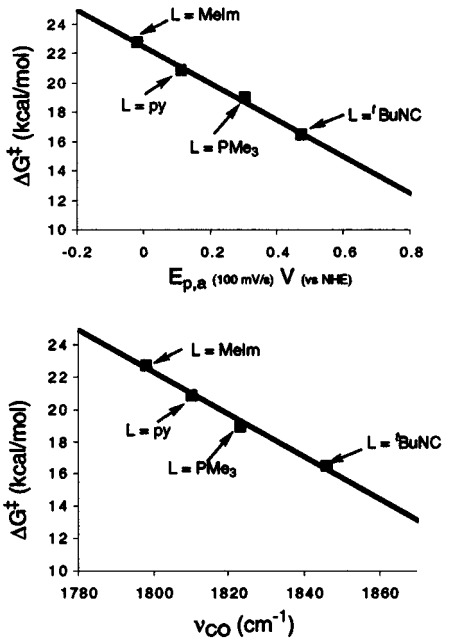

Figure 1. Correlation of activation energies for interfacial migration and electronic properties of TpRe(CO)(L)(η^2-furan) systems ($E_{p,a}$ measured at 100 mV/s and reported in cases where $E_{1/2}$ values were unobtainable).

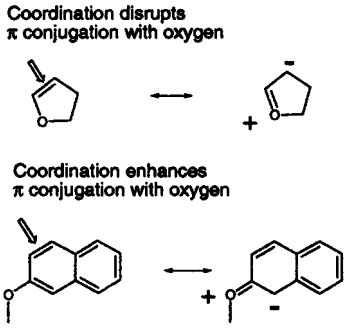

Figure 2. Comparison of relative rates of interfacial isomerization for several monocyclic and bicyclic arenes, furans, and dihydrofurans.

isomerization (>20.8 kcal/mol) is likely due to the increase in double-bond character between C3 and C4 for the free ligand relative to naphthalene as a result of an interaction of the methoxy group with C1 and C2 (Figure 2). With a greater localization of the C1−C2 double bond, the complex would be expected to act more like an olefin and have a higher barrier to the face-flip mechanism than its parent naphthalene. Indeed, the relative rates of substitution for the 1,8-dimethylnaphthalene and 2-methoxynaphthalene complexes of {TpRe(CO)(^{t}BuNC)} in acetone show the latter substitutes more slowly than the former (vide infra). Applying this logic in reverse, a vinyl ether would be expected to have a lower barrier for a face-flip for a given metal system than its olefin counterpart because the ground state for the complexed vinyl either is higher in energy than that for the olefin (Scheme 8). This accounts for the 5 kcal/mol difference in $\Delta G^{\ddagger}$ for the interfacial isomerizations of the dihydrofuran complexes **19** and **20**.

Intrafacial Migrations. The intrafacial migration of coordinated aromatic ligands of the pentaammineosmium(II) system has been studied previously; however, mechanistic analysis of these complexes was somewhat limited in scope due to the achiral nature of the $\{Os(NH_3)_5\}^{2+}$ fragment.[1] The intrafacial migration of the complex $[Os(NH_3)_5(\eta^2\text{-benzene})]^{2+}$ has been determined as 1×10^4 s^{-1} at 20 °C, corresponding to an activation barrier of ~12 kcal/mol. Intrafacial migration of the anisole complex $[Os(NH_3)_5(\eta^2\text{-anisole})]^{2+}$ from the 2,3-η^2 to the 5,6-η^2 isomer has been found to be 0.9 s^{-1} at 20 °C, resulting in a $\Delta G^{\ddagger}$ of ~17 kcal/mol.[37] A summary of rates and activation energies for intrafacial migration of several $[Os(NH_3)_5(\eta^2\text{-aromatic})]^{2+}$ complexes is listed in Table 3. In comparison to the osmium system, the {TpRe(CO)(MeIm)} fragment has a somewhat higher barrier for intrafacial migration of benzene (~2 kcal/mol). Presumably, this increase is due to the more electron-rich nature of the rhenium center ($E_{p,a}$ for the rhenium benzene complex **16** is about 300 mV more negative than that of its osmium analogue). However, $\Delta G^{\ddagger}$ values of ring-walk for the osmium and rhenium anisole systems are almost identical, presumably due to the steric interactions of the methoxy substituent and the ligand set of the rhenium system. For both $[Os(NH_3)_5(\eta^2\text{-anisole})]^{2+}$ and TpRe(CO)(MeIm)(η^2-anisole), the activation energy was measured for the migration from the 2,3-η^2 to the 5,6-η^2 isomer. The upper limit of $\Delta G^{\ddagger}$ for intrafacial migration (5,6-η^2 to 7,8-η^2) of the complex $[Os(NH_3)_5(\eta^2\text{-2-methylnaphthalene})]^{2+}$ is comparable[1] to those observed for the naphthalene complexes of the {TpRe(CO)(py)}and {TpRe(CO)(MeIm)} fragments (**12** and **15**). In contrast, the lower limit for this migration is almost 2 kcal/mol greater than the observed barrier for TpRe(CO)(^{t}BuNC)(η^2-naphthalene) (**4**). These data roughly correlate with the expected electronic characteristics obtained from cyclic voltammetry of the relevant osmium and rhenium systems. As a comparison, a recent study by Perutz et al. has shown the activation barrier for the intrafacial migration of the rhodium(I) system CpRh(PMe$_3$)(η^2-naphthalene) to be 17.8 kcal/mol.[38]

Table 3. Rates and Activation Energies for Intrafacial Migrations of $[Os(NH_3)_5(\eta^2\text{-L}_{Ar})]^{2+}$ Complexes at 20 °C

compound	k (s^{-1})	$\Delta G^{\ddagger}$ (kcal/mol)
$[Os(NH_3)_5(\eta^2\text{-benzene})]^{2+}$	10000	12
$[Os(NH_3)_5(\eta^2\text{-anisole})]^{2+}$	0.9[a]	17
$[Os(NH_3)_5(\eta^2\text{-2-methyl-naphthalene})]^{2+}$	$0.001 < k < 1$[b]	$21 > \Delta G^{\ddagger} > 17$
$[Os(NH_3)_5(\eta^2\text{-1-methylpyrrole})]^{2+}$	100	14

[a] Refers to migration from 2,3-η^2 to 5,6-η^2 isomer. [b] Refers to migration from 5,6-η^2 to 7,8-η^2 isomer. (Data taken from ref 1.)

A graph similar to that obtained for the interfacial migration of the TpRe(CO)(L)(η^2-furan) systems is presented for the intrafacial migration of the various naphthalene systems (**4**, **12**, and **15**) in Figure 3. Again, a linear correlation is observed between the activation free energy and the II/I reduction potentials ($E_{p,a}$ at 100 mV/s) and the carbonyl stretching frequencies as L is varied. In this case, only three data points could be obtained for the ring-walk mechanism since the TpRe(CO)(PMe$_3$)(η^2-naphthalene) system (**9**) is observed as single diastereomer.[10]

Within a given {TpRe(CO)(L)} family, several trends become apparent in the activation free energies observed for the intrafacial process. For the {TpRe(CO)(MeIm)} system, the values for $\Delta G^{\ddagger}$ are higher for the intrafacial migration of the furan and thiophene complexes relative to those for the pyrrole analogue. This difference is likely to be due to several factors. The 3,4-η^2 intermediates implicated for the ring-walk mechanism of the heterocycles may be less stable for the oxo and thiomethine ylides compared to the azamethine ylide intermediate for the pyrrole complex **18** (see Scheme 7). Of note, pyrrole

(37) Harman, W. D.; Sekine, M.; Taube, H. *J. Am. Chem. Soc.* **1988**, *110*, 5725.
(38) Cronin, L.; Higgit, C. L.; Perutz, R. N. *Organometallics* **2000**, *19*, 672.

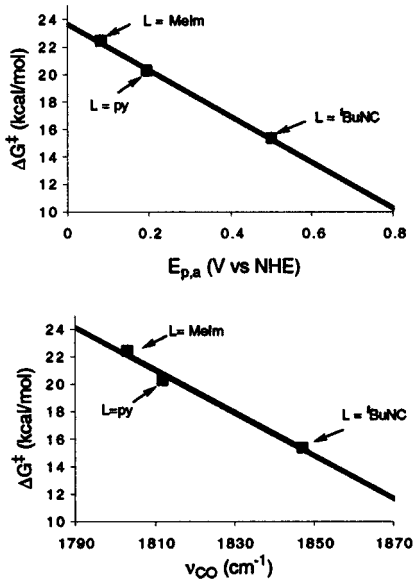

Figure 3. Correlation of activation energies for intrafacial migration and electronic properties of TpRe(CO)(L)(η^2-naphthalene) systems ($E_{p,a}$ measured at 100 mV/s and reported in cases where $E_{1/2}$ values were unobtainable).

complexes of the pentaammineosmium(II) system have been shown to readily undergo 1,3-dipolar cycloadditions, whereas the furan and thiophene complexes have never been observed to react in this manner.[39] The slower rate of intrafacial migration for thiophene and furan ligands may simply be a reflection of the greater stability of their π-bound isomers. Whereas the 1-methylpyrrole complex (**18**) undergoes substitution in acetone with a half-life of about 1.5 h at 20 °C, the thiophene (**14**) and furan (**13**) complexes have substitution half-lives of >3 h at 100 °C. Assuming similar substitution mechanisms, this observation suggests that the O and S heterocycle complexes have a greater thermal stability than the pyrrole complex (**18**). The low values of $\Delta G^{\ddagger}$ for intrafacial isomerization (10 kcal/mol) and the half-life of substitution for **18** can also be attributed in part to the methyl group of the heterocycle that interacts with the ancillary ligands of the rhenium. In a similar manner, the 2,5-dimethylpyrrole complex of osmium(II) undergoes a much more rapid intrafacial isomerization than the corresponding parent pyrrole complex.[39]

The absence of fluxionality in the spectra of the 2-substituted furan and naphthalene systems of {TpRe(CO)(tBuNC)} is a direct result of the supression of intrafacial migrations for these systems; however, the 2-methylthiophene system has access to a lower energy S-bound intermediate, whereas complex **2** does not (vide supra). In comparing various thiophene analogues, another important trend emerges in the relative amounts of η^2- and S-bound isomers of thiophene. The ratio of η^2:η^1 isomers for **3** is 1.2:1 but for **8** is 5.2:1, indicating that the η^2-bound isomer is favored for more electron-rich metal systems. For the pyridine and 1-methylimidazole analogues, the putative S-bound isomer cannot be detected, nor can it be for the pentaammineosmium(II) analogue. This trend was first postulated by Angelici for benzothiophene.[40]

Both the kinetic stability of TpRe(CO)(L)(η^2-L_{Ar}) complexes with regard to ligand dissociation and the rate of linkage isomerization are related to the electronic properties of the metal.

(39) Gonzalez, J.; Koontz, J. I.; Myers, W. H.; Hodges, L. M.; Sabat, M.; Nilsson, K. R.; Neely, L. K.; Harman, W. D. *J. Am. Chem. Soc.* **1995**, *117*, 3405.

(40) Angelici, R. J. *Coord. Chem. Rev.* **1990**, *105*, 61.

Table 4. Rates and Free Energies of Activation for Decomposition of TpRe(CO)(L)(η^2-furan) and TpRe(CO)(L)(η^2-naphthalene) Complexes in Acetone

compound	$t_{1/2}$ (h)	k (h^{-1})[a]	T (K)	$\Delta G^{\ddagger}$ (kcal/mol)[b]
TpRe(CO)(tBuNC)(η^2-furan) (**1**)	42.5	0.016	298	24.6
TpRe(CO)(PMe_3)(η^2-furan) (**7**)	168	0.0041	296	23.3
TpRe(CO)(py)(η^2-furan) (**10**)	1.87	0.37	373	28.8
TpRe(CO)(MeIm)(η^2-furan) (**13**)	2.85	0.38	373	29.0
TpRe(CO)(tBuNC)(η^2-naphthalene) (**14**)	12.1	0.057	296	23.8
TpRe(CO)(py)(η^2-naphthalene) (**12**)	0.69	1.00	373	28.1
TpRe(CO)(MeIm)(η^2-naphthalene) (**15**)	1.31	0.60	373	28.5

[a] Error in rate estimated to be ±4%. [b] Error in activation energy estimated to be ±1 kcal/mol.

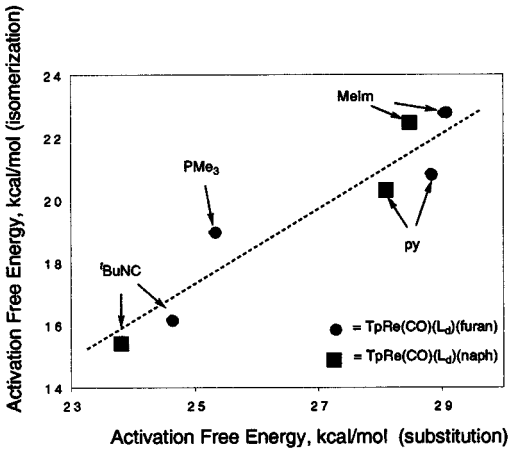

Figure 4. Correlation of free energies of activation for ligand dissociation (in acetone) versus interfacial migration of TpRe(CO)(L)-(η^2-furan) (●) and intrafacial migration of TpRe(CO)(L)(η^2-naphthalene) (■).

Thus, a direct correlation between these two properties is also expected. In Table 4, substitution data are listed for various TpRe(CO)(L)(η^2-furan) and TpRe(CO)(L)(η^2-naphthalene) complexes, and a plot of the isomerization rate and the substitution rate (expressed as free energies of activation) is presented in Figure 4. The correlation between the free energies of activation for isomerization and dissociation is clearly not as strong as the correlation of free energies for migration versus electronic properties of the rhenium (vide supra). The reason for the poor correlation may involve steric effects which play a more important role in dissociation than in migration. In addition, entropic effects may affect the activation energies for dissociation. Thus, while we assume that any temperature-dependent component of the activation energy for the isomerizations is minimal (vide supra), this assumption may not hold in the case of dissociation. Nevertheless, the fact that a general correlation between the two types of activation energies (substitution and isomerization) is observed indicates that the electronic characteristics of the rhenium centers play an important role in both dissociation and migration of the metal center.

Conclusions

The {TpRe(CO)(L)} metal fragments have been shown to bind in a dihapto fashion a variety of aromatic ligands including arenes, aromatic heterocycles, and polycyclic aromatics. Moreover, these chiral rhenium systems have demonstrated an ability to differentiate enantiofaces of prochiral aromatic ligands. The diastereoselectivities exhibited by the TpRe systems are modest

and vary depending on the identity of L and the aromatic ligand. Furthermore, the interconversion of the facial diastereomers of the TpRe(CO)(L)(η^2-L_{Ar}) systems has been found to be nondissociative in nature and to proceed through both interfacial and intrafacial migrations. The free energies of activation for interfacial migration, intrafacial isomerization, and substitution correlate with the electron density of the metal (as indicated by both electrochemical and infrared absorption data). Thus, for a metal−alkene complex, both interfacial and intrafacial isomerizations can be lower energy processes than substitution, and weakening the olefin−metal bond can induce either process. In the case of an electron-rich metal where back-bonding is prominent, lowering the electron density of the metal facilitates these isomerizations. In addition, the rates of ligand dissociation as well as the rates of intra- and interfacial migration correlate with the degree of localization of the π bond prior to complexation. Thus, complexes of aromatic ligands show much shorter half-lives to substitution and to interfacial isomerization than their olefinic counterparts. Finally, the relative amounts of S-bound and η^2-bound isomers for thiophene directly correlate with the electronic properties of the metal, the latter being favored by a more electron-rich metal system.

Experimental Section

All ^{1}H NMR spectra were recorded in acetone-d_6 on a Varian INOVA-500 spectrometer at a variety of temperatures. For spectra recorded at conditions other than ambient temperature, the sample was allowed to equilibrate to the set temperature for approximately 10 min. Separate T_1 and spin saturation measurements were then performed on the same sample. For the spin saturation experiments, an off-resonance decoupled spectrum was obtained as a control spectrum, while other spectra were collected in which specific peaks of interest were irradiated. The ratio of the peak intensities in the irradiated and off-resonance decoupled spectra and the measured T_1 values were used in eq 1 to give the rate of migration. A delay time of $5T_1$ was utilized for each spin saturation experiment. From this value and the set temperature, the values for the activation energy were calculated by using eq 2.

Error Analysis. Errors in both rate (k) and activation energy ($\Delta G^{\ddagger}$) measurements were calculated by using the following equation:[41]

$$\delta q = \sqrt{\left(\frac{\partial q}{\partial x}\delta x\right)^2 + \cdots + \left(\frac{\partial q}{\partial z}\delta z\right)^2} \qquad (4)$$

The values used for the uncertainties represent either the standard deviations for a series of values (e.g., multiple $M(O)/M(\infty)$ values for more than one signal of a ^{1}H NMR pattern) or the standard uncertainty of a particular measurement (e.g., the temperature of an NMR experiment to the nearest degree). The errors were found to be approximately 5% of the calculated values. Utilizing the error calculated for the rate constant determinations and an error of ± 1 °C, the error associated with the $\Delta G^{\ddagger}$ values was estimated to be ± 0.3 kcal/mol.

Acknowledgment. This work was supported by the NSF (CHE9807375) and the NIH (R01-GM49236). We thank Robert G. Bryant and Jeff Ellena for their helpful insights.

Supporting Information Available: Synthetic procedures and full characterization data for all compounds (PDF). This material is available free of charge via the Internet at http://pubs.acs.org.

JA003195J

(41) Taylor, J. R. *An Introduction to Error Analysis The Study of Uncertainties in Physical Measurements*; Oxford University Press: Mill Valley, CA, 1982.